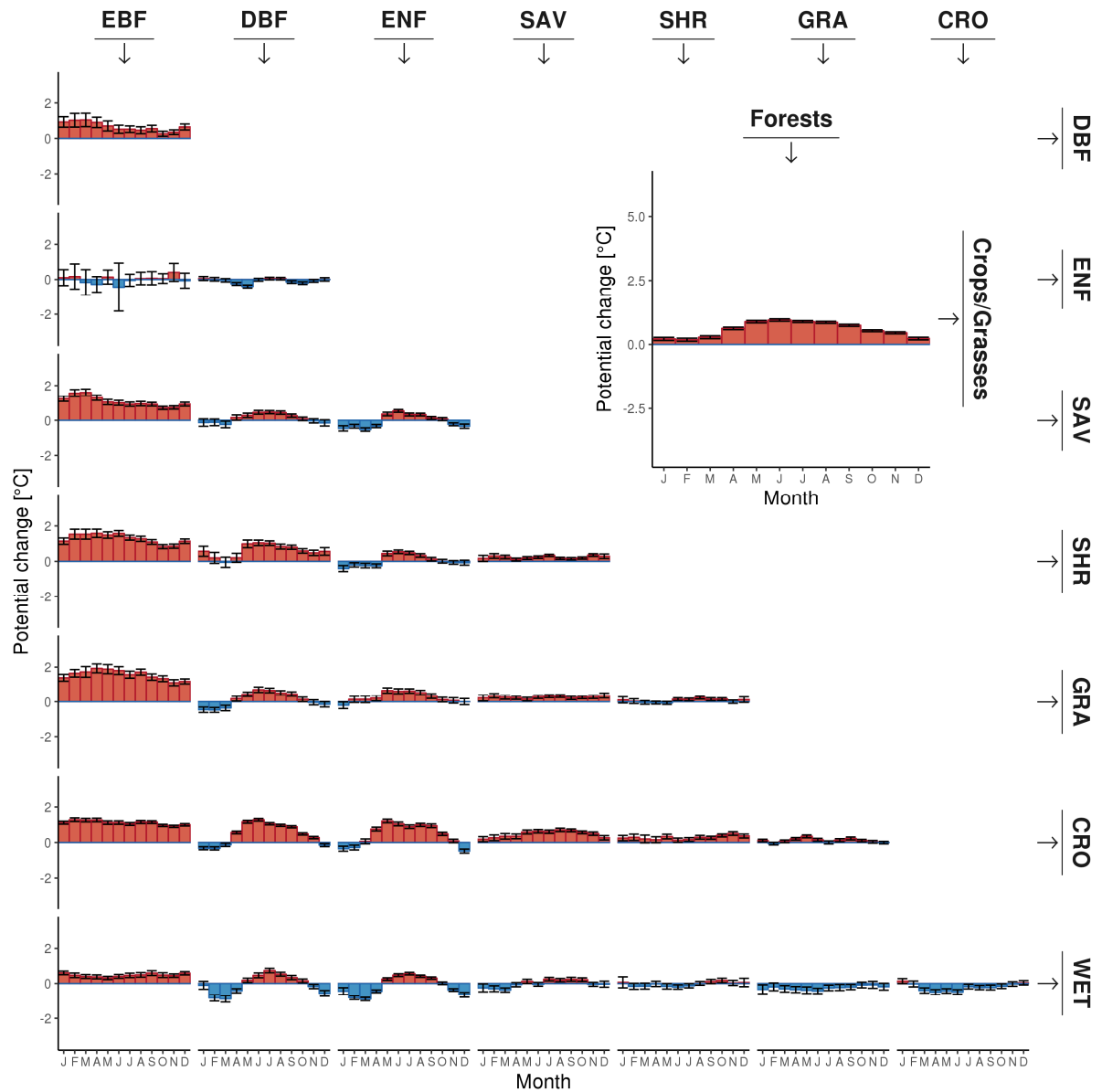
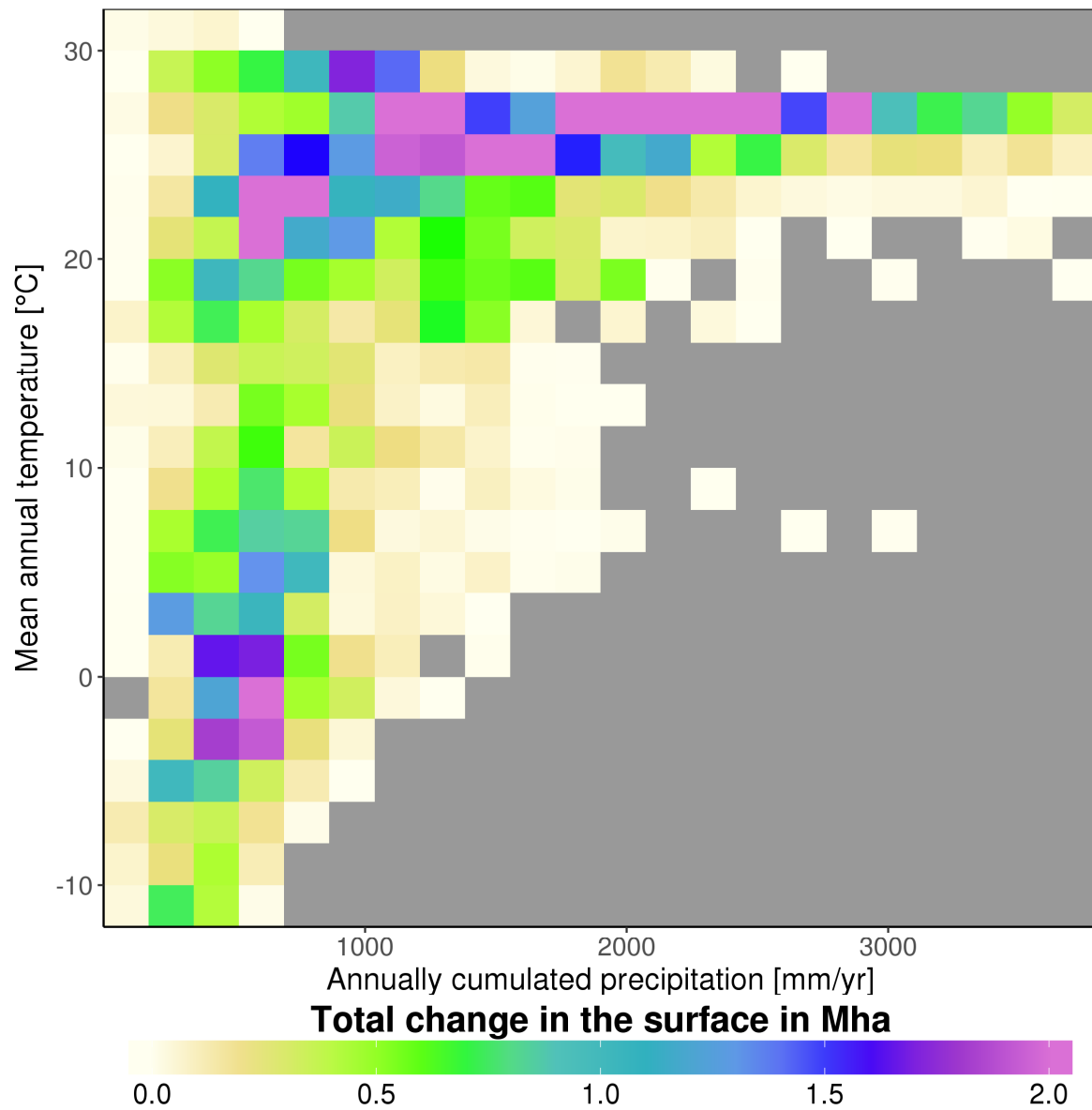


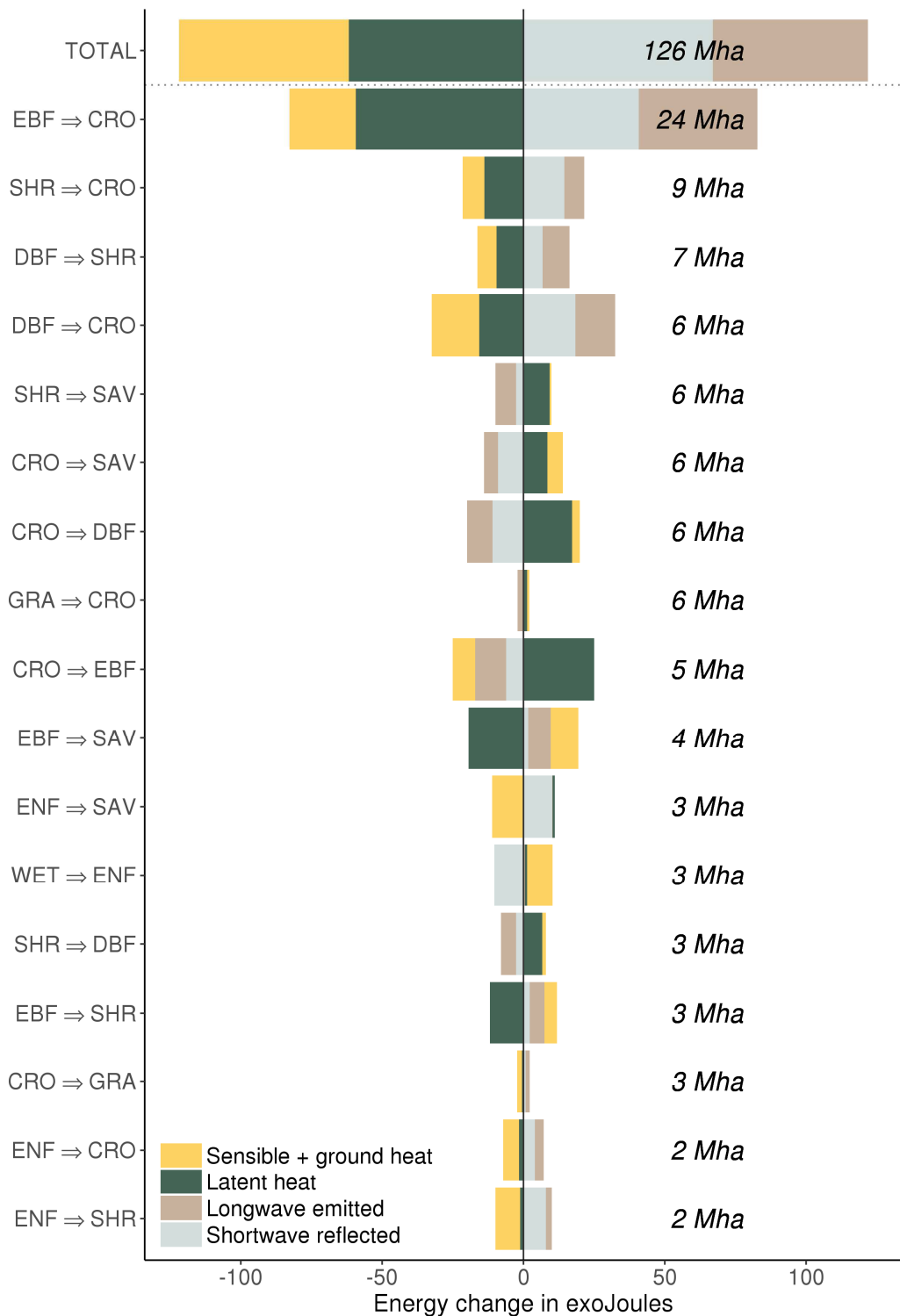
**Supplementary Figure 1 | Global summary of the seasonal potential change in surface energy balance for various transitions in vegetation type as derived from satellite observations.** The transitions shown involve the following vegetation classes: evergreen broadleaf forests (EBF), deciduous broadleaf forests (DBF), evergreen needleleaf forests (ENF), savannas (SAV), shrublands (SHR), grasslands (GRA), croplands (CRO) and wetlands (WET). Because transitions are symmetric, reverse transitions can be derived by inverting the sign. The inset shows a more generic transition from Trees to either Crops or Grasses corresponding to the maps shown in Figures 1 and 2 of the main text. Letters in the x-axis represents the months of the year.



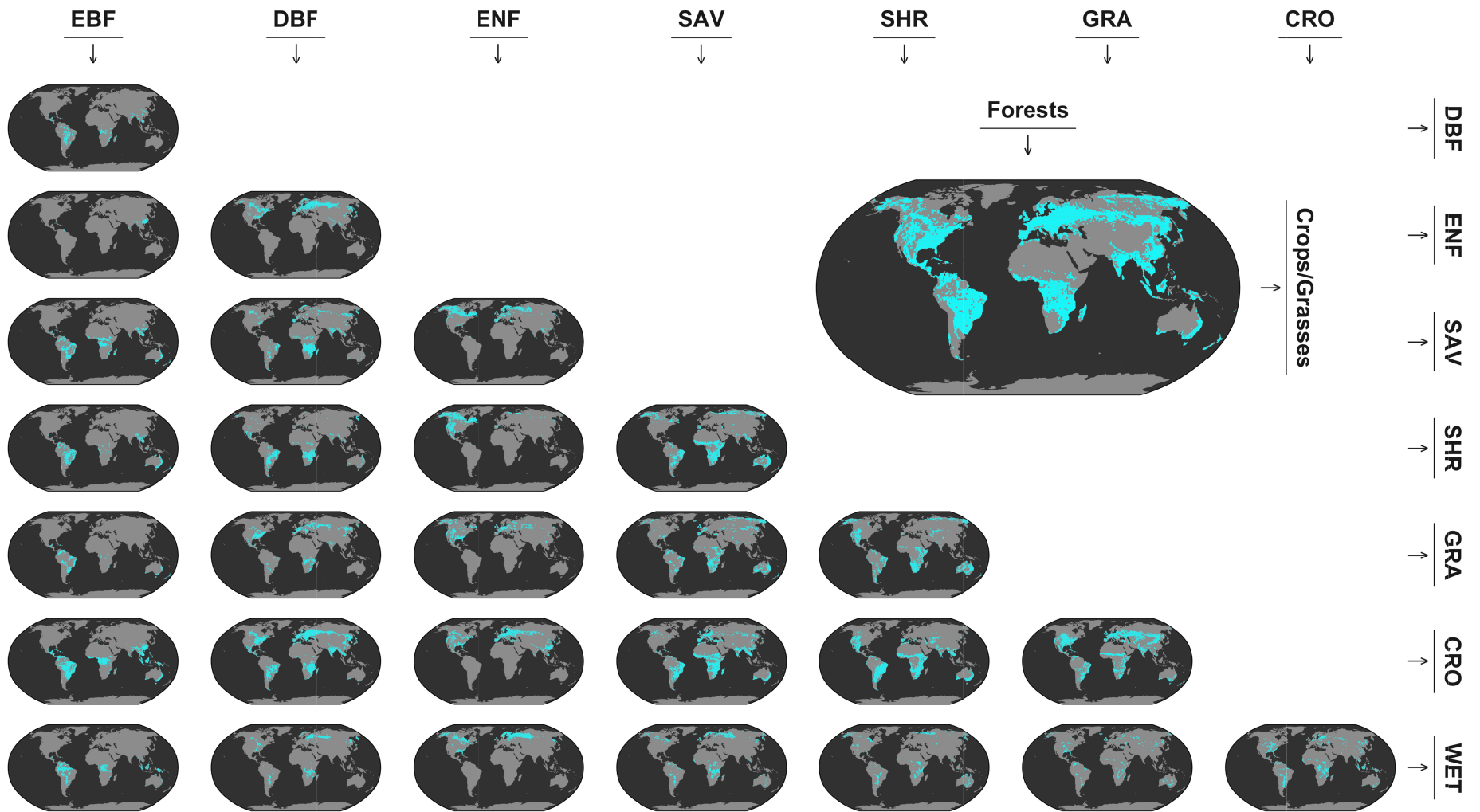
**Supplementary Figure 2 | Global summary of the seasonal potential change in mean land surface temperature for various transitions in vegetation type as derived from satellite observations.** For descriptions of the vegetation classes, see Supplementary Figure 1. Letters in the x-axis represents the months of the year. The confidence interval represents plus or minus two times the standard error around the mean.



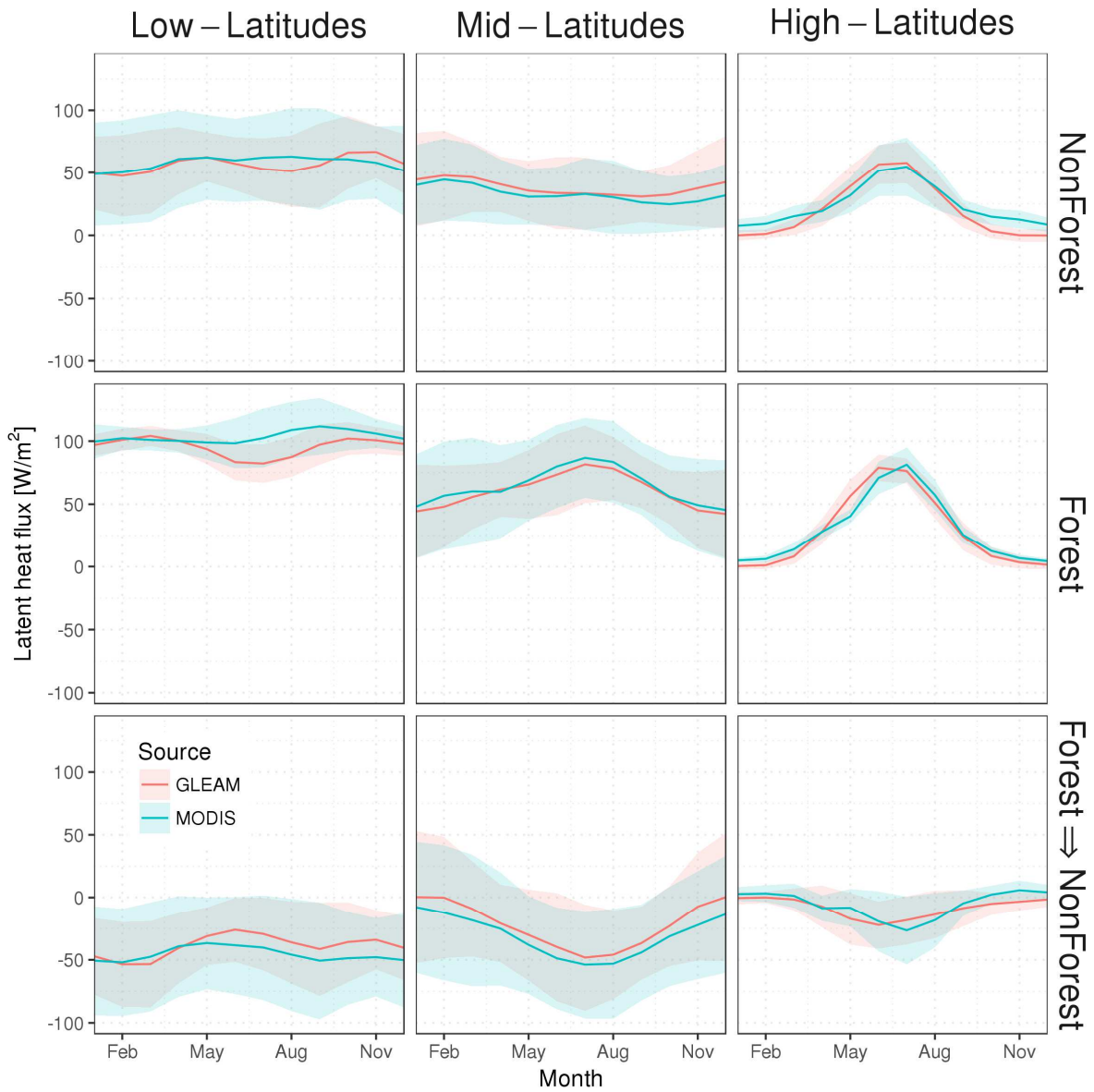
**Supplementary Figure 3 | Total change in area from 2000 to 2015 under different climate gradients.** Change relates to all vegetation transitions considered in this study together, according to the ESA CCI land cover maps<sup>1</sup>. The climate axes are calculated based on CRU data v4.00 at  $0.5^\circ \times 0.5^\circ$  resolution.



**Supplementary Figure 4 | Cumulated changes in energy for each component of the surface energy balance resulting from major vegetation transitions that occurred between 2000 and 2015.** Transitions are sorted according to decreasing changed area. The changed area per transition, calculated based on the ESA CCI land cover maps<sup>1</sup>, are reported in megahectares on the right of the bars. The transitions shown involve the following vegetation classes: evergreen broadleaf forests (EBF), deciduous broadleaf forests (DBF), evergreen needleleaf forests (ENF), savannas (SAV), shrublands (SHR), grasslands (GRA), croplands (CRO) and wetlands (WET).



**Supplementary Figure 5 | Areas where data is available in the final dataset for different vegetation transitions.** For descriptions of the vegetation classes, see Supplementary Figure 1.



**Supplementary Figure 6 | Inter-comparison of the latent heat flux products.** The MODIS MOD16A2 product<sup>2</sup> used in the main paper is compared against the GLEAM v3.1 product<sup>3,4</sup> for all pixels at 1°spatial resolution with high forest cover (>75%) against those with low forest cover (<25%). Forest cover is derived from the ESA CCI land cover map<sup>1</sup> of 2010.



## References

1. ESA. *Land Cover CCI Product User Guide Version 2*. (2017). at <[http://maps.elie.ucl.ac.be/CCI/viewer/download/ESACCI-LC-Ph2-PUGv2\\_2.0.pdf](http://maps.elie.ucl.ac.be/CCI/viewer/download/ESACCI-LC-Ph2-PUGv2_2.0.pdf)>
2. Mu, Q., Heinsch, F., Zhao, M. & Running, S. W. Development of a global evapotranspiration algorithm based on MODIS and global meteorology data. *Remote Sens. Environ.* **106**, 285–304 (2007).
3. Miralles, D. G. *et al.* Global land-surface evaporation estimated from satellite-based observations. *Hydrol. Earth Syst. Sci.* **15**, 453–469 (2011).
4. Martens, B. *et al.* GLEAM v3: Satellite-based land evaporation and root-zone soil moisture. *Geosci. Model Dev.* **10**, 1903–1925 (2017).
5. Di Gregorio, A. *Land Cover Classification System (LCCS). Classification concepts and user manual. Software version 2*. (2005). at <<http://www.fao.org/docrep/008/y7220e/y7220e00.HTM>>
6. Poulter, B. *et al.* Plant functional type classification for Earth System Models: results from the European Space Agency's Land Cover Climate Change Initiative. *Geosci. Model Dev.* **8**, 2315–2328 (2015).